



# Progress Towards Mammalian Whole-Brain Cellular Connectomics

Shawn Mikula\*

Max-Planck Institute for Neurobiology, Electrons - Photons - Neurons, Martinsried, Germany

Neurons are the fundamental structural units of the nervous system—i.e., the Neuron Doctrine—as the pioneering work of Santiago Ramón y Cajal in the 1880's clearly demonstrated through careful observation of Golgi-stained neuronal morphologies. However, at that time sample preparation, imaging methods and computational tools were either nonexistent or insufficiently developed to permit the precise mapping of an entire brain with all of its neurons and their connections. Some measure of the “mesoscopic” connective organization of the mammalian brain has been obtained over the past decade by alignment of sparse subsets of labeled neurons onto a reference atlas or via MRI-based diffusion tensor imaging. Neither method, however, provides data on the complete connectivity of all neurons comprising an individual brain. Fortunately, whole-brain cellular connectomics now appears within reach due to recent advances in whole-brain sample preparation and high-throughput electron microscopy (EM), though substantial obstacles remain with respect to large volume electron microscopic acquisitions and automated neurite reconstructions. This perspective examines the current status and problems associated with generating a mammalian whole-brain cellular connectome and argues that the time is right to launch a concerted connectomic attack on a small mammalian whole-brain.

## OPEN ACCESS

### Edited by:

James A. Bourne,  
Australian Regenerative Medicine  
Institute, Australia

### Reviewed by:

Alessandra Angelucci,  
University of Utah, USA  
Bryan William Jones,  
University of Utah, USA

### \*Correspondence:

Shawn Mikula  
mikula@neuro.mpg.de

**Received:** 25 January 2016

**Accepted:** 26 May 2016

**Published:** 30 June 2016

### Citation:

Mikula S (2016) Progress Towards  
Mammalian Whole-Brain Cellular  
Connectomics.  
*Front. Neuroanat.* 10:62.  
doi: 10.3389/fnana.2016.00062

**Keywords:** whole-brain, sample preparation, ultramicrotomy, electron microscopy, connectomics

## INTRODUCTION

Perception, cognition and behavior are consequences of neural computations executed by neuronal circuits that are widely distributed throughout the whole-brain. Since its inception, neuroscience has attempted to interpret brain organization and function without a detailed map of its total neuronal constituents and their complete inter-connectivities at the required synaptic resolution. Without such a map, a whole-brain cellular connectome, it is highly improbable that the precise neural computations underlying brain and behavior will ever be adequately understood. Currently only electron microscopy (EM) provides the resolution necessary to reliably reconstruct all neuronal circuits contained within a given volume in terms of individual synapses, though continued improvements in super-resolution light microscopy may one day provide a suitable alternative. A comprehensive reconstruction of a whole-brain synaptic “wiring diagram” based on high-throughput EM is thus highly desirable.

Several reviews covering cellular connectomics have appeared in recent years (Lichtman and Sanes, 2008; Lichtman and Denk, 2011; Denk et al., 2012; Helmstaedter, 2013; Peddie and Collinson, 2014; Wanner et al., 2015). A discussion of the progress and problems specifically associated with whole-brain cellular connectomics has not yet appeared. Here I discuss the concrete steps that can lead to a cellular connectome of a small mammalian whole-brain.

## THE CRITICAL STEPS

There are a number of steps necessary for reconstructing the mammalian whole-brain neural circuit *in toto* (Figure 1).

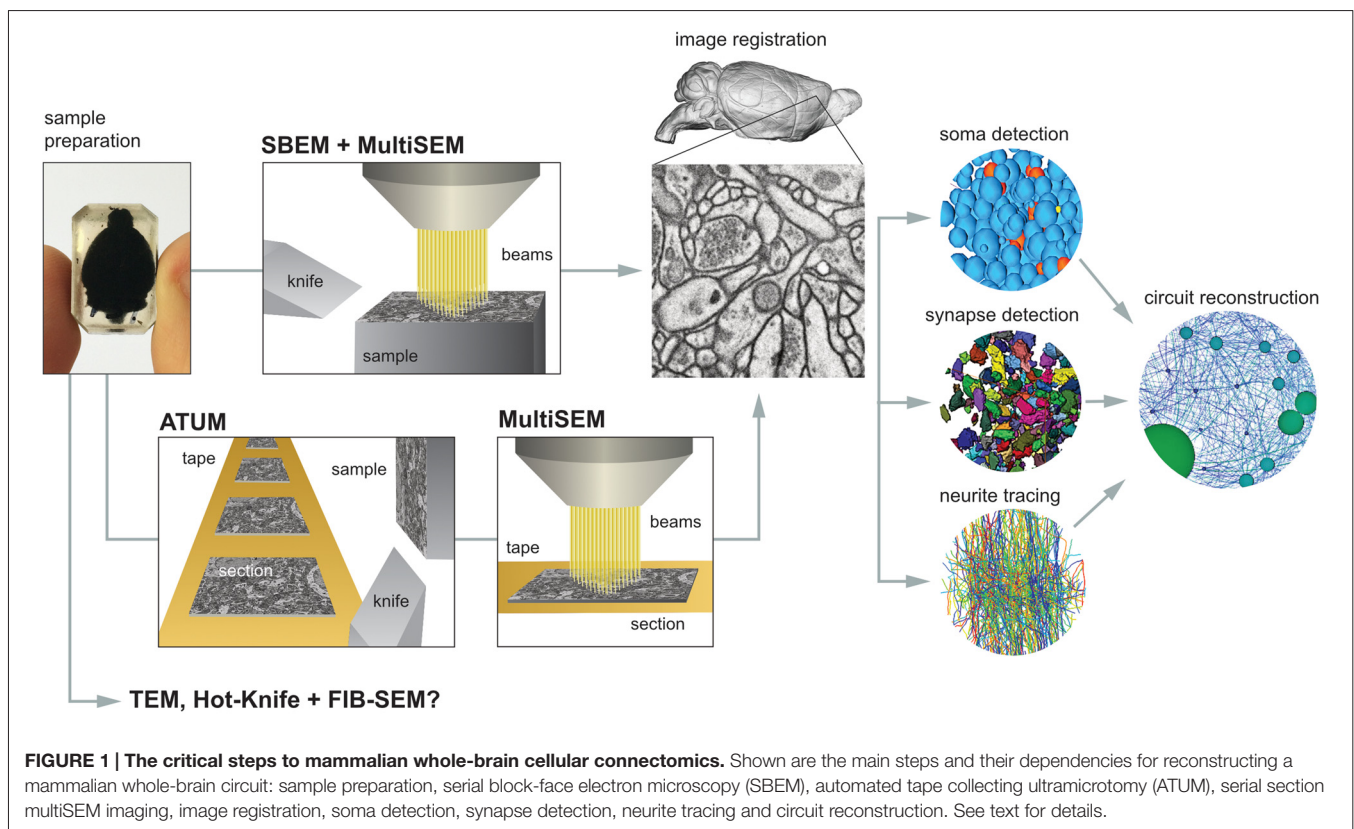
### Sample Preparation

The first step in the process is the sample preparation. Perfusions of whole-brains with osmium tetroxide solutions were performed in the 1960's but were not entirely successful as white matter was not completely stained, nor was whole-brain plastic embedding employed (Palay et al., 1962). Recently, whole mouse brain staining and embedding employing diffusion was described. The BROPA method (Brain-wide formamide-Reduced-Osmium staining with Pyrogallol-mediated osmium Amplification) results in the preservation and staining of the cellular ultrastructure throughout the brain at a resolution sufficient for reliably tracing neurites and identifying synapses, which are both necessary and sufficient for the reconstruction of brain-wide neuronal circuits (Mikula and Denk, 2015). Further improvements of the BROPA method and its application to larger species (e.g., rat, marmoset and macaque) are currently underway.

X-ray micro-computed tomography (i.e., X-ray microCT) is one method for non-invasively imaging whole brains at the micro-scale, which is suitable for assessing brain integrity (e.g., detection of sample cracks and dissection-related damage) and stain uniformity. X-ray microCT relies on the detection of transmitted X-rays (i.e., projections) through a thick sample.

A series of X-ray projections from a range of angles is then used for tomographic reconstruction by converting image data in the Radon transform domain to a volume dataset in the spatial domain (Paulus et al., 2000). Since the contrast obtained from X-ray microCT is similar to that of volume EM (Mikula and Denk, 2015; Dyer et al., 2016), it may be considered a downsampled version of the volume EM dataset. Typical resolutions from commercial X-ray microCT systems range from 10 to 15 microns for small mammalian whole-brain samples prepared for EM. The use of brighter, coherent light sources (e.g., synchrotron radiation) can improve resolution in these samples down to one micron or possibly better (Dyer et al., 2016), though it is currently unclear whether these resolution gains will be sufficient for mammalian whole-brain cellular connectomics.

Volume visualization of an X-ray microCT dataset of an adult Etruscan pygmy shrew and mouse brain prepared for EM demonstrates completely intact brains (Figures 2A,B). Recent EM dataset volumes (blue) from Briggman et al. (2011), Bock et al. (2011), and Kasthuri et al. (2015), are shown adjacent to the mouse brain for comparison. Sagittal and coronal slices through an X-ray microCT dataset for the pygmy shrew and mouse brain confirm the absence of cracks and complete, uniform staining (Figures 2C,D). Scanning electron microscopy (SEM) of the striatum of the pygmy shrew and mouse brain (Figures 2E,F) demonstrates ultrastructural preservation and high membrane contrast that, in the mouse where it has been quantified, appears sufficient for reconstructing even the finest neuronal processes and synapses (Mikula and Denk, 2015).



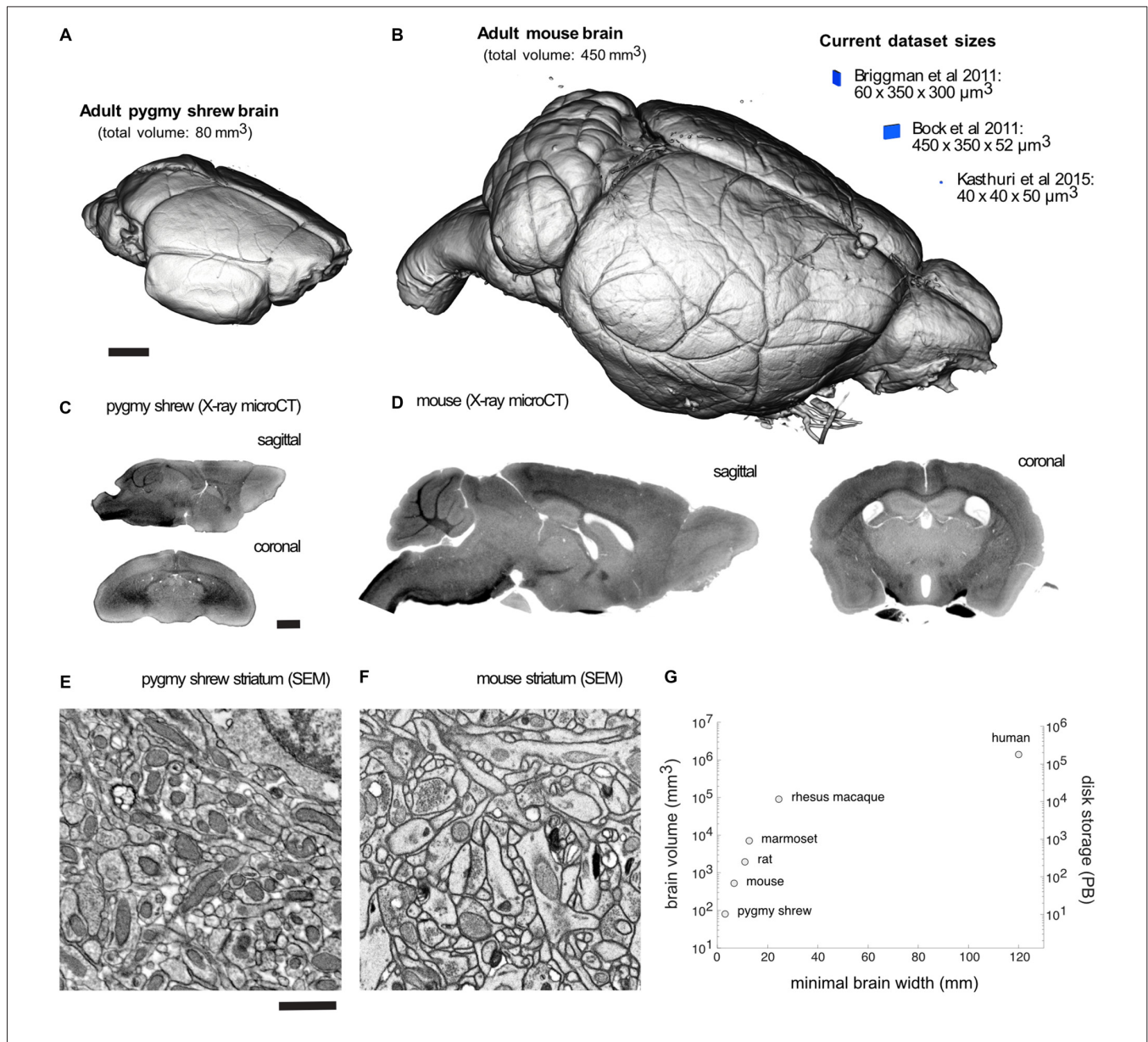


**FIGURE 2 | Mammalian whole-brain sample preparation for electron microscopy (EM).** Volume visualization of an X-ray microCT dataset of an adult (A) pygmy shrew and (B) mouse brain prepared for EM using a Brain-wide formamide-reduced-osmium staining with pyrogallol-mediated osmium amplification (BROPA)-like protocol (Mikula and Denk, 2015). Recent EM dataset volumes (blue), all less than 0.01 mm<sup>3</sup>, are shown adjacent to the mouse brain for comparison. Sagittal and coronal slices through an X-ray microCT dataset for the (C) pygmy shrew and (D) mouse brain. Scanning electron micrographs from the striatum of the (E) pygmy shrew and (F) mouse brain shown in (A,B), respectively. (G) Scatter plot of mammalian brain volumes, disk storage requirements, assuming 20 nm isotropic voxel size, and minimal brain width, which is important for diamond knife cutting requirements. Imaging parameters in (E,F) are similar to those from Mikula and Denk, 2015. X-ray microCT and EM image intensities are inverted. Scale bars are 1 mm in (A,C), and 1 μm in (E). Scale bar in (A) applies to (B), (C) applies to (D), (E) applies to (F).

## Volume EM

There are two routes available for high-throughput, large-volume EM, using either serial block-face electron microscopy (SBEM, Figure 1; Denk and Horstmann, 2004; Briggman et al., 2011) or automated tape-collecting ultramicrotomy (ATUM; Hayworth et al., 2006; Schalek et al., 2011). In SBEM, an SEM in-chamber ultramicrotome sequentially removes ultrathin sections from the sample, exposing a new surface (i.e., block-face) on the sample,

which is then imaged by SEM. The removed sections are neither collected nor imaged and can pose a debris problem in the SEM if not properly handled. In ATUM, serial sections are produced on a standard ultramicrotome and collected automatically on tape, which is subsequently imaged via SEM.

The primary technical challenge for whole-brain SBEM is the design of the in-chamber microtome and nano-positioning machines with sufficient precision and stiffness, whereas the

main challenge using ATUM involves the reliable collection of thin, intact, wrinkle- and chatter-free sections. To image a whole-brain using a conventional single-beam microscope is impractical; thus both volume EM imaging routes critically depend on multi-beam SEM (multi-SEM), a recent advance in imaging technology (Eberle et al., 2015; Kemen et al., 2015), to achieve the throughput (i.e., >1 GHz image acquisition rate, inclusive of stage movement overhead) necessary for imaging mammalian whole-brains within an acceptable period of time at a resolution sufficient for reconstructing neuronal circuits (e.g., 20 nm, isotropic).

Additional potential routes for mammalian whole-brain volume EM cannot be ruled out (**Figure 1**). For example, TEM (Bock et al., 2011; Marc et al., 2013) or combined Hot-Knife and FIB-SEM (Hayworth et al., 2015) may allow for parallel imaging, though in place of multiple e-beams, multiple TEMs or FIB-SEMs are required. However, due to the slower imaging throughputs, 5–8 MHz for TEM (Bock et al., 2011; Lee et al., 2016) and 1 MHz for FIB-SEM (Hayworth et al., 2015), roughly 100–200 TEMs or 1000 FIB-SEMs would be required to match the imaging throughput of a single multiSEM, which can exceed 1 GHz (Kemen et al., 2015), making TEM or FIB-SEM approaches apparently less cost effective and practical.

Volume EM of the smallest adult mammalian brains, Etruscan pygmy shrew or bumblebee bat, with an estimated brain volume of approximately 80 mm<sup>3</sup>, requires about 3 months, whereas the adult mouse brain at 450 mm<sup>3</sup> requires 1.5 years, using a 1 GHz image acquisition rate and 20 nm voxel size. In principle, imaging times can be substantially reduced by the addition of more beams to the multi-SEM, allowing for more than an order of magnitude reduction in imaging times, thus providing a viable solution to imaging larger brains (e.g., rat, marmoset, even human).

## Data Storage

The decision to store whole-brain volume EM data on spinning disks or tape media will depend largely on the trade-off between data access rates vs. storage capacity cost, though additional factors such as reliability, security and mobility may be considered. For the smallest mammalian brains (i.e., Etruscan pygmy shrew or bumblebee bat), the cost for the 10 PB storage required (**Figure 2G**), imaged at 20 nm isotropic voxel, is about 100 k Euros for tape storage vs. 500 k Euros for disk, assuming current estimates of 0.01 Euro/GB for tape storage and 0.05 Euro/GB for disk. For a mouse whole-brain, storage requirements increase to 56 PB and tape storage costs to 560 k Euros (or 2.8 million Euros for disk), which are well within current institutional capabilities and funding. For the human brain, however, the expected 175 Exabytes storage requirement (**Figure 2G**), costing 1.75 billion Euros for tape (or 8.75 billion Euros for disk), will likely exceed individual institutions, thus requiring collective efforts.

## Image Registration

The assembly of 2D images into a registered 3D volume is a largely solved problem and several acceptable solutions exist (Guest and Baldock, 1995; Saalfeld et al., 2010; Tasdizen et al., 2010). In the case of SBEM, the registration problem is

substantially simpler due to the general absence of nonlinear distortions in the images, requiring only the estimation of image translational offsets determined using a similarity measure such as cross-correlation that is subsequently used to obtain a global least squares solution of the linear system of image offset equations (Denk and Horstmann, 2004; Briggman et al., 2011; Mikula et al., 2012). In addition, the use of X-ray microCT whole-brain data as 3D “ground truth” is expected to substantially facilitate the EM image registration.

## Image Post-Processing and Circuit Reconstruction

There are three steps that can begin in parallel once registered volume EM data becomes available. For soma and synapse detection, reliable methods have been developed that generally involve classification of image feature vectors with additional post-processing (Kreshuk et al., 2011; Morales et al., 2011; Becker et al., 2013; Tek et al., 2014; Márquez Neila et al., 2016). For neurite tracing or segmentation, though progress has been made (Jain et al., 2010; Kaynig et al., 2013; Liu et al., 2014; Perez et al., 2014; Plaza et al., 2014; Berning et al., 2015; Ai-Awami et al., 2016) the problem remains unsolved. Crowd-sourcing efforts that rely on manual neurite tracing (Arganda-Carreras et al., 2015) are currently used for annotating small-volume EM datasets (see **Figure 2B**, Current dataset sizes) but will not scale to larger volumes such as small mammalian whole-brains. For example, given the estimate of 5 h/mm manual neurite tracing speed from Berning et al. (2015), it would take more than 500,000 years to manually trace all neurites in the mouse brain (assuming 100 million neurons with an average neurite length per neuron of 10 mm) and 50 billion Euros (assuming 10 Euros/h). Fortunately, there are alternatives on the horizon. Whether the solution comes from deep machine learning methods currently being used in SEM (Huang and Jain, 2013), from autotracing methods originally developed for light microscopy (Ming et al., 2013) and applied to cellular boundary probability maps, or from elsewhere remains to be seen.

Can image processing demands keep pace with imaging acquisition throughput? This is a complicated question due to the multiple possible post-processing strategies that can be deployed. For example, it is likely that distributed image registration and reliable nuclei and synapse detection can be performed before image data is written to disk or tape, where subsequent retrieval would prove costly in terms of image read times. If this is not possible and image data is written to disk or tape before registration and additional post-processing, then subsequent computations requisite for registration and segmentation may prove to be a bottleneck. In any event, the large petabyte-scale EM volumes characteristic of small mammalian whole-brains are not expected to pose an insurmountable computer processing problem as block-based segmentations of large EM datasets have recently been demonstrated (Kroeger et al., 2013) and it is expected that such block-based approaches, in conjunction with CPU-GPU clusters for high-performance computing, will accommodate even mammalian whole-brain EM datasets.

Once somas and synapses are autodetected and neurites are autotraced, the final step of neuronal circuit reconstruction

involves assigning the detected synapses to pre- and post-synaptic neurites, assigning neurites to connecting somas and by the transitive relation, connecting synapses to their pre- and post-synaptic somas.

## REAL AND POTENTIAL ISSUES

### General Technical Considerations

There are a number of problems that are expected with the approach described here besides the need for algorithms capable of reliable neurite autotracing as discussed in the preceding section. The long duration of the volume EM acquisitions will pose a challenge. In the case of the mouse brain, the estimated 1.5 years required for volume EM data acquisition is an order of magnitude longer than current volume EM acquisitions (Bock et al., 2011; Briggman et al., 2011), which necessitates the ability to pause the acquisition as soon as a problem, such as component failure, is detected, correct the problem and then restart the acquisition without any data loss. The complexity of the multiSEM and nanopositioning machines will make this a challenge as there are many components that can fail or malfunction. Unintended diamond knife damage and likely inevitable dulling, both requiring knife replacement, are problems that may prove difficult to overcome if hundreds of thousands of consecutive thin sectionings are required. In this regard, non-mechanical approaches to removing material, such as ion milling, offer a distinct advantage, though their suitability to multiSEM secondary electron (SE) imaging has not yet been demonstrated and may be problematic due to ion beam-induced surface streaking. In addition, since EM necessarily involves irradiating a sample with electrons (typically at high currents, such as nA), sample charging is a common problem in high-vacuum conditions, resulting in information loss and image aberrations, though using in-chamber evaporative coating with metals (Titze and Denk, 2013) or including or synthesizing *en bloc* conductive polymers can address this problem.

### Validation of Circuit Reconstructions

An important issue is validation of the reconstructed brain-wide circuits. While consensus of redundantly- and manually-traced neurites and annotated synapses is one approach (Helmstaedter et al., 2011; Mikula and Denk, 2015), it relies on model-based assumptions. A more convincing route may involve comparison of EM-based circuit reconstructions with light microscopic reconstructions of sparse labeling in the same animal, such as may be obtained with monosynaptic deletion-mutant rabies virus (Wickersham et al., 2006). Another route may involve imaging a sub-volume at a higher resolution, such as 2–5 nm, in order to assess whether all small synapses and fine neurites can be reliably detected and annotated throughout the full volume acquired at a coarser resolution of 10–20 nm. Although recent results suggest that 10 nm in-plane resolution and 30 nm slice thickness are sufficient for reliable circuit reconstructions in whole mouse brain preparations (Mikula and Denk, 2015), further validation of these results in different areas of the brain is prudent. It should be noted that different sample preparations and volume imaging

methods are expected to have different resolution requirements for circuit reconstruction (e.g., Mishchenko et al., 2010).

### Missing Neurochemistry and Gap Junctions

To what extent will a whole-brain cellular connectome obtained from EM permit inferences about neuronal function? Do we need detailed neurochemical information or is ultrastructure in addition to known cell-type neurochemical information sufficient? Certainly the existence of silent synapses (Atwood and Wojtowicz, 1999), gap junctions, more than 50 chemically-distinct neurotransmitters and myriad receptor subtypes with widely-varying post-synaptic responses would urge caution (see Bargmann and Marder, 2013).

Gap junctions deserve special emphasis since they are prevalent in mammalian brains (Rozental et al., 2000) and at least for *C. elegans*, form networks that are not correlated with synaptic networks (Varshney et al., 2011). Unfortunately, gap junctions are generally difficult to reliably identify in conventional EM preparations (Varshney et al., 2011) and may necessitate the use of modified sample preparations for enhanced gap junction staining (van Deurs, 1975; Baker et al., 1985) or the preservation of the extracellular space, which provides indirect evidence for their presence (Cragg, 1980; Pallotto et al., 2015).

It must be emphasized that ultrastructural maps of whole-brain synaptic connectivity likely do not contain all requisite information for accurate whole-brain simulations but we will not know for certain what additional neurochemical information is needed until we are in possession of such connectional maps from mammalian whole-brains, the lessons of the *C. elegans* nervous system and crustacean stomatogastric ganglia notwithstanding. Additional neurochemical information will likely necessitate the development of novel, high-throughput imaging methods beyond the scope of the ultrastructural approach described here. Nonetheless, we may ask, how far can mammalian whole-brain ultrastructure inform us about function and behavior? We are now in a position to find out.

## PROSPECTIVE

### Realising Cajal's Vision

The Neuron Doctrine, established in the 1880's (Ramón y Cajal, 1889), has been central to our understanding of neuronal circuit organization and has led to inferences over neuronal function; e.g., direction of information flow in the hippocampal circuit (Ramón y Cajal, 1995). The methods in Ramon y Cajal's time were clearly inadequate to map the connections between all neurons in a mammalian whole-brain, but today we are in possession of the tools required to realize this vision, bringing the neuroanatomical program he initiated to completion.

### What will a Mammalian Whole-Brain Circuit Diagram Tell Us?

The only nervous system whose circuitry has been completely mapped is that of the worm, *C. elegans* (White et al., 1986; Emmons, 2015). From this precedent, we can be

confident that a mammalian whole-brain neuronal connectivity map will not only inspire and guide countless neuroscience investigations but will also contribute to a better understanding of the neuronal basis of brain, behavior and ultimately, ourselves. But what, specifically, will a mammalian whole-brain circuit diagram tell us? Besides indicating pathways for information flow and the possibility of testing competing neuronal computational models, a complete mammalian whole-brain circuit map will allow us to revisit the concept of the “brain area”, an abstraction whose usefulness in early sensori-motor processing stages is generally accepted due to the topographic mapping of sensory receptors and motor effectors, but whose utility in higher stages of processing is far from clear. Historically, architectonic differentiation, cytochemical signatures and physiological properties have been used to demarcate brain areas (Felleman and Van Essen, 1991), though these approaches are vulnerable to subjective bias (but see Schleicher et al., 1999). More recently, spatial clustering of gene expression patterns has been used (Hawrylycz et al., 2011), though the clusters generally demarcate cortical lamina and not areal boundaries. A mammalian whole-brain circuit diagram will allow us to revisit the brain

area concept by providing a precise connective basis for potential brain parcellations and abstractions and is expected to allow us to see the brain, not as a collection of discrete brain areas or cell types with interconnections, but as a complicated network of individual neurons that may defy simplification.

## AUTHOR CONTRIBUTIONS

SM performed the experiments and analysis and wrote the article.

## FUNDING

Supported by the Max Planck Society.

## ACKNOWLEDGMENTS

I thank Winfried Denk for providing an ideal environment and for many helpful discussions, Sarah Mikula for helpful feedback over the manuscript, Julia Kuhl for help with figures, and Michael Brecht and Saikat Ray for providing aldehyde-fixed Etruscan pygmy shrew brains.

## REFERENCES

- Ai-Awami, A. K., Beyer, J., Haehn, D., Kasthuri, N., Lichtman, J. W., Pfister, H., et al. (2016). Neuroblocks—visual tracking of segmentation and proofreading for large connectomics projects. *IEEE Trans. Vis. Comput. Graph.* 22, 738–746. doi: 10.1109/TVCG.2015.2467441
- Arganda-Carreras, I., Turaga, S. C., Berger, D. R., Cireşan, D., Giusti, A., Gambardella, L. M., et al. (2015). Crowdsourcing the creation of image segmentation algorithms for connectomics. *Front. Neuroanat.* 9:142. doi: 10.3389/fnana.2015.00142
- Atwood, H. L., and Wojtowicz, J. M. (1999). Silent synapses in neural plasticity: current evidence. *Learn. Mem.* 6, 542–571. doi: 10.1101/lm.6.6.542
- Baker, T. S., Sosinsky, G. E., Caspar, D. L., Gall, C., and Goodenough, D. A. (1985). Gap junction structures. VII. Analysis of connexon images obtained with cationic and anionic negative stains. *J. Mol. Biol.* 184, 81–98. doi: 10.1016/0022-2836(85)90045-2
- Bargmann, C. I., and Marder, E. (2013). From the connectome to brain function. *Nat. Methods* 10, 483–490. doi: 10.1038/nmeth.2451
- Becker, C., Ali, K., Knott, G., and Fua, P. (2013). Learning context cues for synapse segmentation. *IEEE Transactions on Medical Imaging*, 32, 1864–1877. doi: 10.1109/TMI.2013.2267747
- Berning, M., Boergens, K. M., and Helmstaedter, M. (2015). SegEM: efficient image analysis for high-resolution connectomics. *Neuron* 87, 1193–1206. doi: 10.1016/j.neuron.2015.09.003
- Bock, D. D., Lee, W.-C. A., Kerlin, A. M., Andermann, M. L., Hood, G., Wetzell, A. W., et al. (2011). Network anatomy and *in vivo* physiology of visual cortical neurons. *Nature* 471, 177–182. doi: 10.1038/nature09802
- Briggman, K. L., Helmstaedter, M., and Denk, W. (2011). Wiring specificity in the direction-selectivity circuit of the retina. *Nature* 471, 183–188. doi: 10.1038/nature09818
- Cragg, B. (1980). Preservation of extracellular space during fixation of the brain for electron microscopy. *Tissue Cell* 12, 63–72. doi: 10.1016/0040-8166(80)90052-x
- Denk, W., Briggman, K. L., and Helmstaedter, M. (2012). Structural neurobiology: missing link to a mechanistic understanding of neural computation. *Nat. Rev. Neurosci.* 13, 351–358. doi: 10.1038/nrn3169
- Denk, W., and Horstmann, H. (2004). Serial block-face scanning electron microscopy to reconstruct three-dimensional tissue nanostructure. *PLoS Biol.* 2:e329. doi: 10.1371/journal.pbio.0020329
- Dyer, E. L., Roncal, W. G., Fernandes, H. L., Gürsoy, D., Xiao, X., Vogelstein, J. T., et al. (2016). Quantifying mesoscale neuroanatomy using X-ray microtomography. *arXiv Preprint arXiv:1604.03629*. Retrieved from: <http://arxiv.org/abs/1604.03629>
- Eberle, A. L., Mikula, S., Schalek, R., Lichtman, J. W., Knothe Tate, M. L., and Zeidler, D. (2015). High-resolution, high-throughput imaging with a multibeam scanning electron microscope. *J. Microsc.* 259, 114–120. doi: 10.1111/jmi.12224
- Emmons, S. W. (2015). The beginning of connectomics: a commentary on White et al. (1986) “The structure of the nervous system of the nematode *Caenorhabditis elegans*”. *Philos. Trans. R. Soc. Lond. B Biol. Sci.* 370:20140309. doi: 10.1098/rstb.2014.0309
- Felleman, D. J., and Van Essen, D. C. (1991). Distributed hierarchical processing in the primate cerebral cortex. *Cereb. Cortex* 1, 1–47. doi: 10.1093/cercor/1.1.1
- Guest, E., and Baldock, R. (1995). Automatic reconstruction of serial sections using the finite element method. *Bioimaging* 3, 154–167. doi: 10.1002/1361-6374(199512)3:4<154::aid-bio2>3.3.co;2-d
- Hawrylycz, M., Ng, L., Page, D., Morris, J., Lau, C., Faber, S., et al. (2011). Multiscale correlation structure of gene expression in the brain. *Neural Netw.* 24, 933–942. doi: 10.1016/j.neunet.2011.06.012
- Hayworth, K., Kasthuri, N., Schalek, R., and Lichtman, J. (2006). Automating the collection of ultrathin serial sections for large volume TEM reconstructions. *Microsc. Microanal.* 12, 86–87. doi: 10.1017/s1431927606066268
- Hayworth, K. J., Xu, C. S., Lu, Z., Knott, G. W., Fetter, R. D., Tapia, J. C., et al. (2015). Ultrastructurally smooth thick partitioning and volume stitching for large-scale connectomics. *Nat. Methods* 12, 319–322. doi: 10.1038/nmeth.3292
- Helmstaedter, M. (2013). Cellular-resolution connectomics: challenges of dense neural circuit reconstruction. *Nat. Methods* 10, 501–507. doi: 10.1038/nmeth.2476
- Helmstaedter, M., Briggman, K. L., and Denk, W. (2011). High-accuracy neurite reconstruction for high-throughput neuroanatomy. *Nat. Neurosci.* 14, 1081–1088. doi: 10.1038/nn.2868
- Huang, G. B., and Jain, V. (2013). Deep and wide multiscale recursive networks for robust image labeling. *arXiv Preprint arXiv:1310.0354*. Retrieved from: <http://arxiv.org/abs/1310.0354>.
- Jain, V., Seung, H. S., and Turaga, S. C. (2010). Machines that learn to segment images: a crucial technology for connectomics. *Curr. Opin. Neurobiol.* 20, 653–666. doi: 10.1016/j.conb.2010.07.004

- Kasthuri, N., Hayworth, K. J., Berger, D. R., Schalek, R. L., Conchello, J. A., Knowles-Barley, S., et al. (2015). Saturated reconstruction of a volume of neocortex. *Cell* 162, 648–661. doi: 10.1016/j.cell.2015.06.054
- Kaynig, V., Vazquez-Reina, A., Knowles-Barley, S., Roberts, M., Jones, T. R., Kasthuri, N., et al. (2013). Large-scale automatic reconstruction of neuronal processes from electron microscopy images. *arXiv: 1303.7186 7186 [cs, Q-Bio]*. Retrieved from: <http://arxiv.org/abs/1303.7186>.
- Kemen, T., Malloy, M., Thiel, B., Mikula, S., Denk, W., Dellemann, G., et al. (2015). “Further advancing the throughput of a multibeam SEM,” in *SPIE Proceedings 9424, Metrology, Inspection, and Process Control for Microlithography* (94241U-94241U-6) (San Jose, CA).
- Kreshuk, A., Straehle, C. N., Sommer, C., Koethe, U., Cantoni, M., Knott, G., et al. (2011). Automated detection and segmentation of synaptic contacts in nearly isotropic serial electron microscopy images. *PLoS One* 6:e24899. doi: 10.1371/journal.pone.0024899
- Kroeger, T., Mikula, S., Denk, W., Koethe, U., and Hamprecht, F. A. (2013). Learning to segment neurons with non-local quality measures. *Med. Image Comput. Comput. Assist. Interv.* 16, 419–427. doi: 10.1007/978-3-642-40763-5\_52
- Lee, W.-C. A., Bonin, V., Reed, M., Graham, B. J., Hood, G., Glattfelder, K., et al. (2016). Anatomy and function of an excitatory network in the visual cortex. *Nature* 532, 370–374. doi: 10.1038/nature17192
- Lichtman, J. W., and Denk, W. (2011). The big and the small: challenges of imaging the brain’s circuits. *Science* 334, 618–623. doi: 10.1126/science.1209168
- Lichtman, J. W., and Sanes, J. R. (2008). Ome sweet ome: what can the genome tell us about the connectome? *Curr. Opin. Neurobiol.* 18, 346–353. doi: 10.1016/j.conb.2008.08.010
- Liu, T., Jones, C., Seyedhosseini, M., and Tasdizen, T. (2014). A modular hierarchical approach to 3D electron microscopy image segmentation. *J. Neurosci. Methods* 226, 88–102. doi: 10.1016/j.jneumeth.2014.01.022
- Marc, R. E., Jones, B. W., Watt, C. B., Anderson, J. R., Sigulinsky, C., and Lauritzen, S. (2013). Retinal connectomics: towards complete, accurate networks. *Prog. Retin. Eye Res.* 37, 141–162. doi: 10.1016/j.preteyeres.2013.08.002
- Márquez Neila, P., Baumela, L., González-Soriano, J., Rodríguez, J.-R., DeFelipe, J., and Merchán-Pérez, Á. (2016). A fast method for the segmentation of synaptic junctions and mitochondria in serial electron microscopic images of the brain. *Neuroinformatics* 14, 235–350. doi: 10.1007/s12021-015-9288-z
- Mikula, S., Binding, J., and Denk, W. (2012). Staining and embedding the whole mouse brain for electron microscopy. *Nat. Methods* 9, 1198–1201. doi: 10.1038/nmeth.2213
- Mikula, S., and Denk, W. (2015). High-resolution whole-brain staining for electron microscopic circuit reconstruction. *Nat. Methods* 12, 541–546. doi: 10.1038/nmeth.3361
- Ming, X., Li, A., Wu, J., Yan, C., Ding, W., Gong, H., et al. (2013). Rapid reconstruction of 3D neuronal morphology from light microscopy images with augmented rayburst sampling. *PLoS One* 8:e84557. doi: 10.1371/journal.pone.0084557
- Mishchenko, Y., Hu, T., Spacek, J., Mendenhall, J., Harris, K. M., and Chklovskii, D. B. (2010). Ultrastructural analysis of hippocampal neuropil from the connectomics perspective. *Neuron* 67, 1009–1020. doi: 10.1016/j.neuron.2010.08.014
- Morales, J., Alonso-Nanclares, L., Rodríguez, J.-R., Defelipe, J., Rodríguez, Á., and Merchán-Pérez, A. (2011). ESPINA: a tool for the automated segmentation and counting of synapses in large stacks of electron microscopy images. *Front. Neuroanat.* 5:18. doi: 10.3389/fnana.2011.00018
- Palay, S. L., McGee-Russell, S. M., Gordon, S. Jr., and Grillo, M. A. (1962). Fixation of neural tissues for electron microscopy by perfusion with solutions of osmium tetroxide. *J. Cell Biol.* 12, 385–410. doi: 10.1083/jcb.12.2.385
- Pallotto, M., Watkins, P. V., Fubara, B., Singer, J. H., and Briggman, K. L. (2015). Extracellular space preservation aids the connectomic analysis of neural circuits. *Elife* 4:e08206. doi: 10.7554/eLife.08206
- Paulus, M. J., Gleason, S. S., Kennel, S. J., Hunsicker, P. R., and Johnson, D. K. (2000). High resolution X-ray computed tomography: an emerging tool for small animal cancer research. *Neoplasia* 2, 62–70. doi: 10.1038/sj.neo.7900069
- Peddie, C. J., and Collinson, L. M. (2014). Exploring the third dimension: volume electron microscopy comes of age. *Micron* 61, 9–19. doi: 10.1016/j.micron.2014.01.009
- Perez, A. J., Seyedhosseini, M., Deerinck, T. J., Bushong, E. A., Panda, S., Tasdizen, T., et al. (2014). A workflow for the automatic segmentation of organelles in electron microscopy image stacks. *Front. Neuroanat.* 8:126. doi: 10.3389/fnana.2014.00126
- Plaza, S. M., Scheffer, L. K., and Chklovskii, D. B. (2014). Toward large-scale connectome reconstructions. *Curr. Opin. Neurobiol.* 25, 201–210. doi: 10.1016/j.conb.2014.01.019
- Ramón y Cajal, S. (1889). Conexión general de los elementos nerviosos. *Med. Pract.* 2, 341–346.
- Ramón y Cajal, S. (1995). *Histology of the Nervous System of Man and Vertebrates. Translated (from the French) by Neely and Larry Swanson*. New York, NY: Oxford University Press.
- Rozental, R., Giaume, C., and Spray, D. (2000). Gap junctions in the nervous system. *Brain Res. Brain Res. Rev.* 32, 11–15. doi: 10.1016/s0165-0173(99)00095-8
- Saalfeld, S., Cardona, A., Hartenstein, V., and Tomančák, P. (2010). As-rigid-as-possible mosaicking and serial section registration of large ssTEM datasets. *Bioinformatics* 26, i57–i63. doi: 10.1093/bioinformatics/btq219
- Schalek, R., Kasthuri, N., Hayworth, K., Berger, D., Tapia, J., Morgan, J., et al. (2011). Development of high-throughput, high-resolution 3D reconstruction of large-volume biological tissue using automated tape collection ultramicrotomy and scanning electron microscopy. *Microsc. Microanal.* 17, 966–967. doi: 10.1017/s1431927611005708
- Schleicher, A., Amunts, K., Geyer, S., Morosan, P., and Zilles, K. (1999). Observer-independent method for microstructural parcellation of cerebral cortex: a quantitative approach to cytoarchitectonics. *Neuroimage* 9, 165–177. doi: 10.1006/nimg.1998.0385
- Tasdizen, T., Koshevoy, P., Grimm, B. C., Anderson, J. R., Jones, B. W., Watt, C. B., et al. (2010). Automatic mosaicking and volume assembly for high-throughput serial-section transmission electron microscopy. *J. Neurosci. Methods* 193, 132–144. doi: 10.1016/j.jneumeth.2010.08.001
- Tek, F. B., Kroeger, T., Mikula, S., and Hamprecht, F. A. (2014). “Automated cell nucleus detection for large-volume electron microscopy of neural tissue” in *Biomedical Imaging (ISBI), 2014 IEEE 11th International Symposium on IEEE (Beijing)*, 69–72. Retrieved from: [http://ieeexplore.ieee.org/xpls/abs\\_all.jsp?arnumber=6867811](http://ieeexplore.ieee.org/xpls/abs_all.jsp?arnumber=6867811)
- Titze, B., and Denk, W. (2013). Automated in-chamber specimen coating for serial block-face electron microscopy. *J. Microsc.* 250, 101–110. doi: 10.1111/jmi.12023
- van Deurs, B. (1975). The use of a tannic acid-glutaraldehyde fixative to visualize gap and tight junctions. *J. Ultrastr. Res.* 50, 185–192. doi: 10.1016/s0022-5320(75)80049-9
- Varshney, L. R., Chen, B. L., Paniagua, E., Hall, D. H., and Chklovskii, D. B. (2011). Structural properties of the caenorhabditis elegans neuronal network. *PLoS Comput. Biol.* 7:e1001066. doi: 10.1371/journal.pcbi.1001066
- Wanner, A. A., Kirschmann, M. A., and Genoud, C. (2015). Challenges of microtome-based serial block-face scanning electron microscopy in neuroscience. *J. Microsc.* 259, 137–142. doi: 10.1111/jmi.12244
- Wickersham, I. R., Finke, S., Conzelmann, K. K., and Callaway, E. M. (2006). Retrograde neuronal tracing with a deletion-mutant rabies virus. *Nat. Methods* 4, 47–49. doi: 10.1038/nmeth999
- White, J. G., Southgate, E., Thomson, J. N., and Brenner, S. (1986). The structure of the nervous system of the nematode *Caenorhabditis elegans*. *Philos. Trans. R. Soc. Lond. B Biol. Sci.* 314, 1–340. doi: 10.1098/rstb.1986.0056

**Conflict of Interest Statement:** The author declares that the research was conducted in the absence of any commercial or financial relationships that could be construed as a potential conflict of interest.

Copyright © 2016 Mikula. This is an open-access article distributed under the terms of the Creative Commons Attribution License (CC BY). The use, distribution and reproduction in other forums is permitted, provided the original author(s) or licensor are credited and that the original publication in this journal is cited, in accordance with accepted academic practice. No use, distribution or reproduction is permitted which does not comply with these terms.